

Vibrational edge modes in intrinsically heterogeneous doped transition metal oxides

I. Martin, E. Kaneshita, and A. R. Bishop

Los Alamos National Laboratory, Los Alamos, New Mexico 87545, USA

R. J. McQueeney

Ames Laboratory, Ames, Iowa 50011, USA

Z. G. Yu

SRI International, Menlo Park, California 94025, USA

(Received 18 August 2004; published 15 December 2004)

By applying an unrestricted Hartree-Fock and a random phase approximation to a multiband Peierls-Hubbard Hamiltonian, we study the phonon mode structure in models of transition metal oxides in the presence of intrinsic nanoscale inhomogeneities induced by hole doping. We identify low-frequency *local* vibrational modes pinned to the sharp interfaces between regions of distinct electronic structure (doped and undoped) and separated in frequency from the band of extended phonons. A characteristic of these “edge” modes is that their energy is essentially insensitive to the doping level. We discuss the experimental manifestations of these modes in inelastic neutron scattering and also in spin and charge excitation spectra.

DOI: 10.1103/PhysRevB.70.224514

PACS number(s): 74.81.-g, 71.38.-k, 61.12.Bt, 63.20.Pw

I. INTRODUCTION

Recent advances in experimental techniques provide strong indications that a broad class of electronic materials, commonly referred to as *strongly correlated*, exhibit intrinsically heterogeneous electronic phases.^{1–8} Strong interactions in these materials drive the phase separation between regions of distinct electronic structure.⁹ However, a competing interaction or electronic kinetic energy can lead to frustration of the global phase separation and to formation of *nanoscale inhomogeneities*, which can take the form of, e.g., stripes and checkerboards¹⁰ or clumps.¹¹ Unlike the conventional spin- and charge-density-wave phases, the ordering of intrinsic heterogeneities is sensitive to thermal and quantum fluctuations,¹² as well as static disorder. This makes an unambiguous identification of such phases and their distinction from the more familiar density-wave instabilities problematic, requiring the development of new diagnostics more sensitive to the unique structure of such phases. Here, we propose one such diagnostic tool which relies on the detection of localized *edge modes* pinned to the interface between regions of different electronic structure. The edge (interface) modes appear in every degree of freedom coupled to the inhomogeneity (charge, spin, lattice),¹³ with corresponding correlated experimental signatures. Here we study the *lattice vibrational edge modes* which lend themselves to study with inelastic neutron scattering. We also compute the corresponding excitation spectra in spin and charge channels and describe the cross correlations.

We focus on one particular class of transition metal oxides that has attracted significant attention recently: namely, cuprates. These are the materials exhibiting high- T_c superconductivity upon doping. The presence of stripes and checkerboards and their possible influence on superconductivity are subjects of intensive debate. Since it appears that stripes can significantly affect superconductivity,^{14–16} it is important to establish whether they are indeed present in the materials.

Our purpose here is to elucidate typical manifestations of stripe order in experimental probes sensitive to the excitations in spin, lattice, and charge sectors. In particular, we compare our theoretical results with the observations of “anomalous” phonon modes in the cuprates.^{17–19} Analogous results also apply to edge mode signatures in other doped transition metal oxides (and related complex electronic materials), as found in recent experimental studies;^{20–24} corresponding modes (phonon shape modes) have already been predicted and identified in conjugated polymers and quasi-one-dimensional (quasi-1D) charge transfer solids.^{25,26}

II. MODEL

To model the CuO_2 planes of doped cuprates, we use a 2D three-band extended Peierls-Hubbard Hamiltonian, which includes both electron-electron and electron-phonon interactions:^{27,28}

$$H_0 = \sum_{\langle ij \rangle \sigma} t_{pd}(u_{ij})(c_{i\sigma}^\dagger c_{j\sigma} + \text{H.c.}) + \sum_{i,\sigma} \epsilon_i(u_{ij})c_{i\sigma}^\dagger c_{i\sigma} + \sum_{\langle ij \rangle} \frac{1}{2} K_{ij} u_{ij}^2 + \sum_{i,j,\sigma,\sigma'} \frac{1}{2} U_{ij} n_{i\sigma} n_{j\sigma'}. \quad (1)$$

Here, $c_{i\sigma}^\dagger$ creates a hole with spin σ on site i ; each site has one orbital ($d_{x^2-y^2}$ on Cu or O p_x or p_y on O). The Cu (O) site electronic energy is ϵ_d (ϵ_p). Here, U_{ij} represents the on-site Cu (O) Coulomb repulsion U_d (U_p) or the intersite one U_{pd} and the summation \sum is taken except for the case $(i,\sigma)=(j,\sigma')$. The electron-lattice interaction causes modification of the Cu–O hopping strength through the oxygen displacement u_{ij} : $t_{pd}(u_{ij})=t_{pd}\pm\alpha u_{ij}$, where $+$ ($-$) applies if the Cu–O bond shrinks (stretches) for a positive u_{ij} ; it also affects the Cu on-site energies $\epsilon_d(u_{ij})=\epsilon_d+\beta\sum_j(\pm u_{ij})$, where the sum runs over the four neighboring O ions. The other

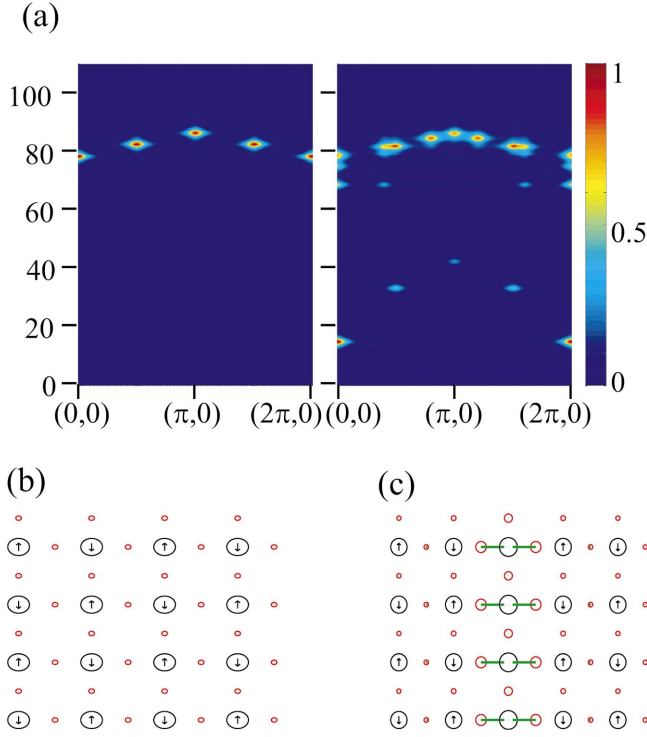


FIG. 1. (a) (Color) Neutron scattering spectra and the ground-state structures for the undoped [left panel in (a) and (b)] and hole-doped (20%) case [right panel in (a) and (c)]. The system sizes are 4×4 and 4×5 , respectively, with periodic boundary conditions. The neutron scattering spectra are symmetrized with respect to directions parallel and perpendicular to the stripe. In the lower plots, black circles represent Cu sites and red circles represent O. The radius of the circle is proportional to the corresponding site hole density. Arrows centered on circles show the magnitude and direction of spin. The green lines originating from O sites indicate the magnitude and direction of the equilibrium O displacements in the presence of a stripe.

oxygen modes couple to electron charge more weakly and are neglected for simplicity. We use the following set of model parameters:^{13,27} $\epsilon_p - \epsilon_d = 4.4$ eV, $U_d = 11$ eV, $U_p = 3.3$ eV, $U_{pd} = 1.1$ eV, $K = 38.7$ eV/Å², $\alpha = 5.2$ eV/Å, and $\beta = 1.2$ eV/Å, with $t_{pd} = 1.1$ eV. To approximately solve the model, we use unrestricted an Hartree-Fock (HF) combined with an inhomogeneous generalized random phase approximation (RPA) for linear lattice fluctuations²⁷ in a supercell of size $N_x \times N_y$ with periodic boundary conditions. In this model, doped holes tend to segregate into stripes due to the competition between the magnetoelastic interaction that favors global electronic phase separation and electronic kinetic energy that favors uniform carrier density.^{29,30} We note that other competing interactions can produce stripes, clumps, and other inhomogeneities;^{31,32} the local, coupled charge-spin-lattice dynamics governing edge modes on these templates then can still be modeled with a similar Hamiltonian and RPA analysis.

The output of the calculation here is the inhomogeneous HF ground state and the phonon eigenfrequencies and eigenvectors. From the phonon eigenmodes, we calculate the corresponding neutron scattering cross section

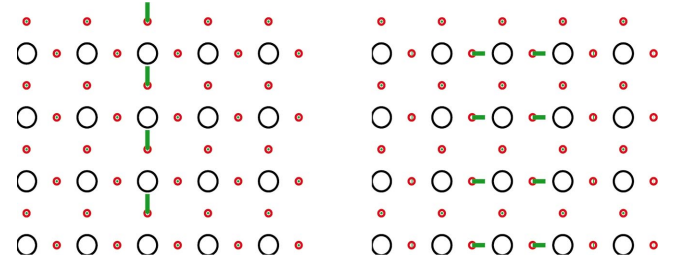


FIG. 2. (Color) Localized vibrational eigenmodes for the case of a 20%-doped CuO_2 plane. The stripe is centered along the middle vertical Cu row. There are two localized branches: One corresponds to the oxygen vibration parallel to the stripe (low frequency, $E = 14.8$ meV, left), and the other corresponds to the oxygen displacements perpendicular to the stripe (high frequency, $E = 68.5$ meV, right). The supercell size is 4×5 .

$$S(\mathbf{k}, \omega) = \int dt e^{-i\omega t} \sum_{ll'} \langle e^{-i\mathbf{k} \cdot \mathbf{R}_l(t)} e^{i\mathbf{k} \cdot \mathbf{R}_{l'}(t)} \rangle, \quad (2)$$

where $\mathbf{R}_l(t) = \mathbf{R}_l^0 + \mathbf{d}_l + \mathbf{u}_l(t)$ is the position of the l th oxygen atom expressed in terms of the location of the unit cell origin \mathbf{R}_l^0 , position within the unit cell \mathbf{d}_l , and time-dependent vibrational component $\mathbf{u}_l(t)$. For phonon modes with $\mathbf{u}_l(t)$ oriented along the corresponding metal-oxygen bonds, on the O_x sublattice $\mathbf{d}_l = (a/2)\hat{x}$ and $\mathbf{u}_l \equiv x_l\hat{x}$, and on the O_y sublattice $\mathbf{d}_l = (a/2)\hat{y}$ and $\mathbf{u}_l \equiv y_l\hat{y}$. The scalar displacements can now be expressed in terms of the normal modes z_n as $x_l(t) = \sum_n \alpha_{x_l,n} z_n(t)$ and $y_l(t) = \sum_n \alpha_{y_l,n} z_n(t)$. Making a first-order expansion in the oxygen displacements, we obtain

$$S(\mathbf{k}, \omega) = \sum_n [k_x^2 |\alpha_{\mathbf{k},n}^x|^2 + k_y^2 |\alpha_{\mathbf{k},n}^y|^2 + k_x k_y (e^{i(k_x - k_y)a/2} \alpha_{\mathbf{k},n}^x \alpha_{-\mathbf{k},n}^y + \text{c.c.})] \times \frac{\hbar}{2m\omega_n} [(1 + n_B) \delta(\omega - \omega_n) + n_B \delta(\omega + \omega_n)]. \quad (3)$$

Here, $\alpha_{\mathbf{k},n}^x = \sum_l e^{-i\mathbf{k} \cdot \mathbf{R}_l^0} \alpha_{x_l,n}$ and $n_B = (e^{\omega_n/T} - 1)^{-1}$ is the thermal population of the phonon mode n . This is a generalization of the usual neutron scattering intensity expression³³ for the case of phonons with a larger real space unit cell. We plot $S(\mathbf{k}, \omega)/|\mathbf{k}|^2$ for \mathbf{k} directions sampling longitudinal modes, consistent with the common experimental convention.

III. LOCAL PHONON MODES

We first analyze the signatures of the edge mode by comparing computed phonon spectra for doped and undoped cuprates (Fig. 1). The predicted neutron scattering intensities are given in the original Brillouin zone, symmetrized with respect to the two possible orientations of the stripe.

The ground-state configuration in the undoped case is a uniform antiferromagnet (AF), while, in the doped (20%) case, the holes partially segregate into a Cu-centered vertical stripe.³⁴ The doping produces *two* quasi-1D low-frequency branches that split off from the band of extended phonon modes characterizing the undoped state. In Fig. 2 we plot

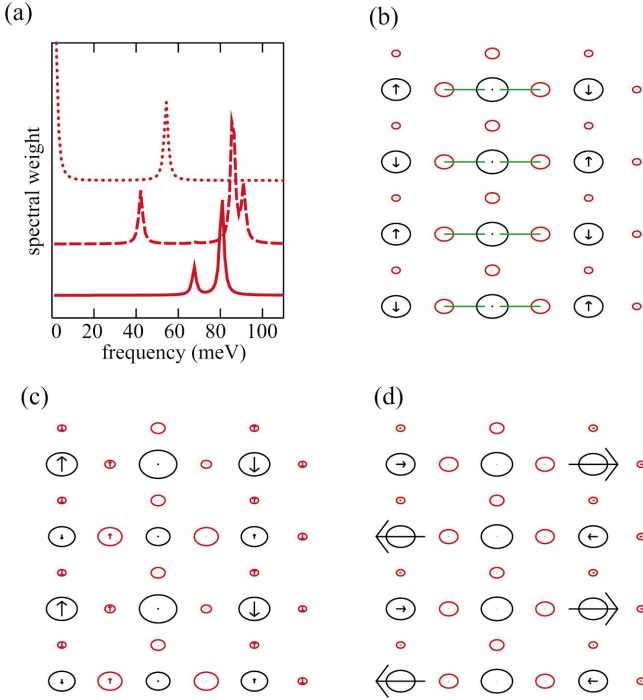


FIG. 3. (Color) Electronic excitations in a 3×4 system with a vertical stripe. (a) Spectral weights of longitudinal magnetic excitation (solid line), transverse magnetic excitation (dotted line), and charge excitation (dashed line) for $(\frac{2}{3}\pi, \pi)$ momentum transfer. The scale for the transverse spin mode is 4000 times larger than the one for others. (b) The ground state. (c) Spin and charge configurations for the excited state ~ 40 meV; this frequency corresponds to the oxygen vibration parallel to the stripe. Here $S_x=0$. (d) S_x configuration for the excited state ~ 50 meV, where $S_z=0$.

representative modes from these branches. Clearly, these are modes “localized” in the direction perpendicular to the stripe. The lower-frequency branch centered around ~ 30 meV corresponds to the oxygen displacements *along* the stripe and the high-frequency one at ~ 70 meV to the vibrations *perpendicular* to the stripe. (The example shown in Fig. 2, right, is a localized asymmetric breathing mode.^{17,18}) The dispersion of the lower branch corresponds to the energy dependence of the localized modes on the quasi-1D momentum along the stripe direction. Different wave vectors cause different degrees of charge transfer between copper and oxygen atoms along the stripe and, hence, have different energies. The dispersion in the direction perpendicular to the stripes is very weak (but nonzero) due to the strong concentration of the modes’ spectral weight along the stripes. Our results are in a semiquantitative agreement with the experiments. By the choice of parameters, we fit the optical phonon band structure in the undoped case. Experimental evidence from neutron scattering^{17,18} shows mode softening of about 15% with doping in the cuprates, consistent with the softening obtained here for the *perpendicular* 70-meV edge mode. Experimentally, the softening is doping independent, which is consistent with the formation of an edge mode, for which the doping is expected to change the intensity but not the energy in the limit of sufficiently dilute stripes. Recent neutron measurements in twinned and de-

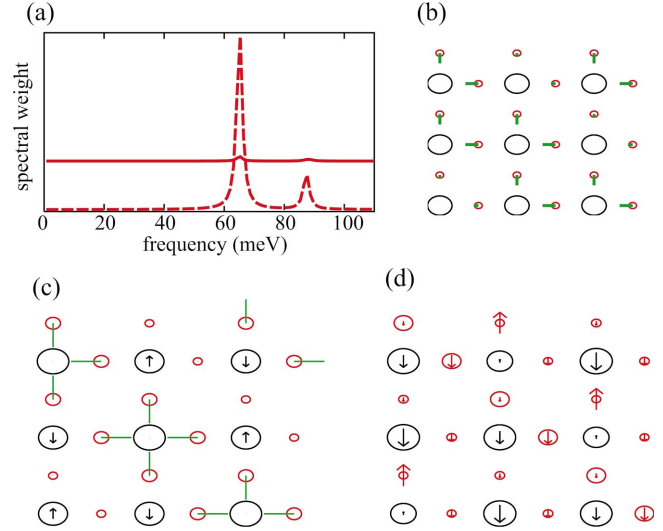


FIG. 4. (Color) Electronic excitations in a 3×3 system with diagonal stripe. (a) Spectral weights of longitudinal magnetic excitations (solid line) and charge excitations (dashed line) for $(\frac{2}{3}\pi, \frac{2}{3}\pi)$ momentum. (b) The phonon mode at 64.3 meV. (c) The ground state and (d) the excited state ~ 65 meV.

twinned $\text{YBa}_2\text{Cu}_3\text{O}_{6+\delta}$ (Ref. 19) have attempted to resolve the phonon spectrum both parallel and perpendicular to the purported stripe direction,³⁵ but conclusive identification has been hampered by the degeneracy and mixing of many modes near the zone boundary. There has been no search yet for the *parallel* edge modes which are predicted here to have a huge softening of $\sim 60\%$. However, there are distinct anomalies in the longitudinal phonon spectrum of $\text{La}_{2-x}\text{Sr}_x\text{CuO}_4$ around 30 meV that have not been studied in detail.¹⁸

Despite the close agreement between the energy scales of the predicted and observed modes, it is important to note some deviations from the reported experimental data for the mode intensities. We speculate that these discrepancies may be due to the detailed local oxygen environments: Either (a) more complex intraunit cell distortions—i.e., local oxygen polarizations (e.g., from local confinement or pairing effects), which would require more detailed modeling than the constrained O displacements used here—or (b) more complex stripe configurations than the regular linear stripes we have considered. (Such textured—e.g., checkerboard—patterns are indeed found in certain models.^{9,32})

IV. MODIFIED ELECTRONIC EXCITATIONS

We now investigate the structure of corresponding electronic excitations in the *charge* and *spin* channels. We again use the inhomogeneous generalized RPA; however, due to the increased computational complexity, we must use smaller system sizes: a 3×3 system for diagonal stripes and a 3×4 system for vertical stripes. In both cases the hole concentration is $\frac{1}{3}$. We have analyzed the spectra, as well as the real-space structure of these excitations. For example, the excitation spectrum in the longitudinal spin channel is given by $I(\omega, q) = \sum_n |\langle 0 | S_z(q) | n \rangle|^2 \delta(\omega - E_n + E_0)$, where $|0\rangle$ and $|n\rangle$

are the Hartree-Fock ground state and an RPA excited state, respectively. The real-space structure of the excitation $|n\rangle$ is described by, e.g., $\langle 0|S_z(i)|n\rangle$. This quantity shows how the expectation value of the z component of spin on site i changes due to the excitation of the RPA state $|n\rangle$ when the system is driven by an external field of frequency $E_n - E_0$.

The phonon spectrum for the vertical 3×4 case is essentially the same as in the 4×5 case in Fig. 1, with two localized branches near 30 meV and 70 meV. However, the relative weight in the localized modes increases with the increased density of stripes. This and the insensitivity of the modes' energy to doping are the main characteristics of the edge modes. For the 3×3 diagonal stripe case, the phonon spectrum has only the high-energy edge mode at 70 meV, but no excitation near 30 meV. Note that the low-energy vibrational mode can only exist for a vertical stripe because the oxygen-mediated charge transfer along the stripe is suppressed in the diagonal case.

The spectra for magnetic and charge excitations for the vertical stripe case are presented in Fig. 3. The spectral weight of the charge excitation at $q = (\frac{2}{3}\pi, \pi)$ has a peak near ~ 40 meV, which corresponds to the frequency of the “half-breathing” oxygen vibration along the stripe [same low-energy branch as Fig. 2(a), but with $q_y = \pi$]. This charge excitation produces dynamic dimerization along the stripe, which couples to the antiphase oxygen vibration parallel to the stripe. On the other hand, the excitation near 70 meV is associated with the antiphase oxygen vibration perpendicular to the stripe [same split-off branch as Fig. 2(b)] and corresponds to the charge excitation at the Cu sites next to the stripe. The transverse spin channel mode at $(\frac{2}{3}\pi, \pi)$ shows not only the Goldstone zero mode but also a higher-energy excitation ~ 50 meV. From Fig. 3(d), this higher-energy excitation likely corresponds to the spin-wave branch folded back at the zone boundary (larger systems sizes are necessary to be definitive.) From continuity of spin-wave excitations, it follows that there is an intensity somewhere below 50 meV at (π, π) . It is possible that this mode has a relation-

ship with the “41-meV” magnetic resonance mode.^{36,37} Note that there is no coupling of magnetic excitations with the low-energy vibrational mode. This is because in the Cu-site-centered stripe, oxygen vibration only transfers charge between the sites with no spin polarization and, hence, does not couple to the spin channel.

Figure 4(a) shows the spectral weights for excitations in the diagonal stripe case. Here, there are several RPA excited states near 65 meV, which lead to a peak in the longitudinal spin excitation spectrum. The excited state that has the lowest energy of the states ~ 65 meV is plotted in Fig. 4(d); the vibrational mode corresponding to this excitation is shown in Fig. 4(b). As discussed earlier, unlike for the vertical stripe case there is no localized vibrational mode around 40 meV, and accordingly there are no RPA spin or charge excitations in this energy range. The only excitations of the longitudinal magnetic and charge channels appear in the 65–90 meV range. The transverse magnetic excitation shows only the Goldstone mode.

V. SUMMARY

We conclude that the formation of split-off *local* modes in spin, charge, and lattice channels, familiar in the polaronic physics of conjugated polymers and quasi-1D charge transfer salts,^{25,26,38} is also expected to be prominently manifested in the case of other doped strongly correlated materials, including nickelates, cuprates, and bismuthates.^{1–8} The intensities of these signatures should increase with doping (and therefore density of interfaces). In addition to angle-resolved photoemission spectroscopy (ARPES) and inelastic magnetic and lattice neutron scattering, experimental techniques that should be applied to study the edge modes include dielectric constants and infrared and Raman spectroscopy²⁵; resonant Raman scattering would be particularly valuable even for low doping levels.²⁶

ACKNOWLEDGMENTS

We would like to acknowledge valuable discussions with T. Egami. This work was supported by the U.S. DOE.

¹J. M. Tranquada, D. J. Buttrey, V. Sachan, and J. E. Lorenzo, Phys. Rev. Lett. **73**, 1003 (1994).

²J. M. Tranquada, J. D. Axe, N. Ichikawa, Y. Nakamura, S. Uchida, and B. Nachumi, Phys. Rev. B **54**, 7489 (1996).

³C. H. Chen, S.-W. Cheong, and A. S. Cooper, Phys. Rev. Lett. **71**, 2461 (1997).

⁴S.-W. Cheong, H. Y. Hwang, C. H. Chen, B. Batlogg, L. W. Rupp, Jr., and S. A. Carter, Phys. Rev. B **49**, 7088 (1994); S.-H. Lee and S.-W. Cheong, Phys. Rev. Lett. **79**, 2514 (1997).

⁵K. Nakajima, Y. Endoh, S. Hosoya, J. Wada, D. Welz, H. M. Mayer, H. A. Graf, and M. Steiner, J. Phys. Soc. Jpn. **66**, 809 (1997).

⁶J. M. Tranquada, B. J. Sternlieb, J. D. Axe, Y. Nakamura, and S. Uchida, Nature (London) **375**, 561 (1995).

⁷J. M. Tranquada, J. D. Axe, N. Ichikawa, A. R. Moodenbaugh, Y. Nakamura, and S. Uchida, Phys. Rev. Lett. **78**, 338 (1997).

⁸A. P. Ramirez, J. Phys.: Condens. Matter **9**, 8171 (1997).

⁹E. Dagotto, T. Hotta, and A. Moreo, Phys. Rep. **344**, 1 (2001); *Intrinsic Multiscale Structure and Dynamics in Complex Oxides*, edited by A. R. Bishop, S. R. Shenoy, and S. Sridar (World Scientific, Singapore, 2003).

¹⁰J. Zaanen and O. Gunnarsson, Phys. Rev. B **40**, 7391 (1989); K. Machida, Physica C **158**, 192 (1989); M. Kato, K. Machida, H. Nakanishi, and M. Fujita, J. Phys. Soc. Jpn. **59**, 1047 (1990).

¹¹A. A. Koulakov, M. M. Fogler, and B. I. Shklovskii, Phys. Rev. Lett. **76**, 499 (1996).

¹²S. A. Kivelson, E. Fradkin, and V. J. Emery, Nature (London) **393**, 550 (1998).

¹³Z. G. Yu, J. Zang, J. T. Gammel, and A. R. Bishop, Phys. Rev. B **57**, R3241 (1998).

¹⁴V. J. Emery, S. A. Kivelson, and O. Zachar, Phys. Rev. B **56**, 6120 (1997).

¹⁵I. Martin, G. Ortiz, A. V. Balatsky, and A. R. Bishop, Int. J. Mod. Phys. B **14**, 3567 (2000).

- ¹⁶A. Bussmann-Holder, K. A. Muller, R. Micnas, H. Buttner, A. Simon, A. R. Bishop, and T. Egami, *J. Phys.: Condens. Matter* **13**, L169 (2001).
- ¹⁷R. J. McQueeney, Y. Petrov, T. Egami, M. Yethiraj, G. Shirane, and Y. Endoh, *Phys. Rev. Lett.* **82**, 628 (1999).
- ¹⁸R. J. McQueeney, J. L. Sarrao, P. G. Pagliuso, P. W. Stephens, and R. Osborn, *Phys. Rev. Lett.* **87**, 077001 (2001).
- ¹⁹L. Pintschovius, W. Reichardt, M. Klser, T. Wolf, and H. v. Lhneysen, *Phys. Rev. Lett.* **89**, 037001 (2003); J.-H. Chung, T. Egami, I. R. J. McQueeney, M. Yethiraj, M. Arai, T. Yokoo, Y. Petrov, H. A. Mook, Y. Endoh, S. Tajima, C. Frost, and F. Dogan, *Phys. Rev. B* **67**, 014517 (2003); D. Reznik, L. Pintschovius, W. Reichardt, Y. Endoh, H. Hiraka, J. M. Tranquada, S. Tajima, H. Uchiyama, and T. Masui, *J. Low Temp. Phys.* **131**, 417 (2003).
- ²⁰J. Tranquada, K. Nakajima, M. Braden, L. Pintschovius, and R. J. McQueeney, *Phys. Rev. Lett.* **88**, 075505 (2002).
- ²¹R. J. McQueeney, J. L. Sarrao, and R. Osborn, *Phys. Rev. B* **60**, 80 (1999).
- ²²M. Braden, W. Reichardt, S. Shiryayev, and S. N. Barilod, *Physica C* **378**, 89 (2002).
- ²³M. d'Astuto, P. K. Mang, P. Giura, A. Shukla, P. Ghigna, A. Mirone, M. Braden, M. Greven, M. Krisch, and F. Sette, *Phys. Rev. Lett.* **88**, 167002 (2002).
- ²⁴J. Zhang, Pengcheng Dai, J. A. Fernandez-Baca, E. W. Plummer, Y. Tomioka, and Y. Tokura, *Phys. Rev. Lett.* **86**, 3823 (2001).
- ²⁵J. T. Gammel, A. Saxena, I. Batistic, A. R. Bishop, and S. R. Phillpot, *Phys. Rev. B* **45**, 6408 (1992).
- ²⁶K. Yonemitsu and A. R. Bishop, *Suppl. Prog. Theor. Phys.* **113**, 155 (1993); B. Scott, S. P. Love, G. S. Kanner, S. R. Johnson, M. P. Wilkerson, M. Berkey, B. I. Swanson, A. Saxena, X. Z. Huang, and A. R. Bishop, *J. Mol. Struct.* **356**, 207 (1995).
- ²⁷K. Yonemitsu, A. R. Bishop, and J. Lorenzana, *Phys. Rev. B* **47**, 12 059 (1993).
- ²⁸Ya-Sha Yi, A. R. Bishop and H. Röder, *J. Phys.: Condens. Matter* **11**, 3547 (1999).
- ²⁹J. Zaanen and P. B. Littlewood, *Phys. Rev. B* **50**, 7222 (1994).
- ³⁰R. J. McQueeney, A. R. Bishop, Ya-Sha Yi, and Z. G. Yu, *J. Phys.: Condens. Matter* **12**, L317 (2000).
- ³¹L. P. Pryadko, S. A. Kivelson, V. J. Emery, Y. B. Bazaliy, and E. A. Demler, *Phys. Rev. B* **60**, 7541 (1999).
- ³²B. P. Stojkovic, Z. G. Yu, A. L. Chernyshev, A. R. Bishop, A. H. Castro Neto, and N. Gronbech-Jensen, *Phys. Rev. B* **62**, 4353 (2000).
- ³³S. W. Lovesy, *Theory of Magnetic Neutron and Photon Scattering* (Oxford University Press, London, 1989).
- ³⁴In the present model the most stable stripe configurations correspond to the insulating stripes with linear filling 1, while experimentally observed stripe periodicity may be more consistent with metallic stripes with filling of approximately 1/2 (Ref. 6). However, for the edge mode properties, we believe, this distinction is not crucial.
- ³⁵H. A. Mook, Pengcheng Dai, F. Dogan, and R. D. Hunt, *Nature (London)* **404**, 729 (2000).
- ³⁶J. Rossat-Mignod, L. P. Regnault, P. Bourges, P. Burlert, C. Vettier, and J. Y. Henryb, *Physica B* **192**, 109 (1993).
- ³⁷C. D. Batista, G. Ortiz, and A. V. Balatsky, *Phys. Rev. B* **64**, 172508 (2001).
- ³⁸K. Fesser, A. R. Bishop, and D. K. Campbell, *Phys. Rev. B* **27**, 4804 (1983).